J. Fluid Mech. (1987), *vol.* 183, *pp.* 365–377
Printed in Great Britain

Linear stability of a cylindrical falling film

By FRANCISCO J. SOLORIO AND MIHIR SEN†
Facultad de Ingeniería, Universidad Nacional Autónoma de México, 04510 México, DF, México

(Received 11 June 1985 and in revised form 16 March 1987)

The problem of a cylindrical falling film, descending vertically outside an infinitely long cylinder is considered. The linear stability of the fully developed flow is studied, first with a perturbation technique for small wavenumbers, and then by direct numerical computation. The numerical results are in agreement with other published values for the cylindrical jet and flat plate limits. The study shows that the cylindrical falling film is unstable for all Reynolds numbers, Weber numbers and radius ratios. Stability and amplification curves are calculated for different values of the parameters. With increasing curvature of the film the range of unstable wavenumbers and the wavenumber of the most amplified wave increase. For low curvature the wavenumber of the most amplified wave decreases with Reynolds number or Weber number, while for high curvatures it increases.

1. Introduction

The stability of gravity-driven flows with free surfaces is important to many industrial processes which include heat and mass exchange through the surface area. Most previous studies have been stability analyses of liquid falling films over an inclined flat plate, in which context a linearized perturbation technique for small wavenumbers was perfected. This includes work by Yih (1954, 1963), Benjamin (1957) and de Bruin (1974). A simple description of the theory is given in the book by Yih (1969).

Several experimental observations of the instability of falling films have been carried out, for instance by Kapitza & Kapitza (1949), Binnie (1957) and more recently by Krantz & Goren (1971) and Pierson & Whitaker (1977). Some, though not all of these, were on falling films around long cylinders. The cylindrical falling film is of importance since many industrial and chemical devices use this type of geometry. In some applications the radius of curvature of the film is not very large with respect to the film thickness. In such cases important differences could arise between the cylindrical-film results and its flat-plate approximation.

Some work relating to the effect of curvature on flow stability has been reported. The classical analysis of a cylindrical water column was by Rayleigh (1879, 1892) with a modern extension given by Chandrasekhar (1961). Theoretical work on cylindrical films was started by Goren (1962) who studied the linear stability of external and internal films to axisymmetric disturbances. However, the study was severely limited by an assumption of zero velocity of the unperturbed flow, under which condition the flow was found to be unstable for small wavenumbers but stable for large ones. Lin & Lui (1975) obtained an evolution equation on which they based their analysis and which is valid only for small wavenumbers and thin films. For this

† Present address: Department of Aerospace and Mechanical Engineering, University of Notre Dame, Notre Dame, IN 46556, USA.

reason their results compare well with those of Kapitza & Kapitza (1949) and Binnie (1957), but not with Goren (1962). Atherton & Homsy (1976) analysed the problem but only to obtain the evolution equations for interfacial waves in two-phase flows, again valid only for small wavenumbers. However, no stability analysis of the steady state was carried out. Krantz & Zollars (1976) started from the Orr–Sommerfeld equation and obtained a series solution in terms of a small wavenumber. Their analysis is valid only for thin films and low Reynolds numbers. In fact their graphs do not consider Reynolds numbers larger than 0.5 which may be important in practice. Homsy & Geyling (1977) studied a slightly different but related problem of a film around a cylinder moving in a vertical direction. But, like Goren (1962), negligible inertia was assumed along with small wavenumbers. More recently, Shlang & Sivashinsky (1982) have obtained an evolution equation using the approximation of strong surface tension. In contrast with previous work, they do not restrict themselves to a linearized analysis nor to axisymmetric flows. Their approach permits the modelling of certain aspects of chaos in the film.

Thus, although some stability results exist for the cylindrical falling film, these have been under a variety of assumptions which have made theoretical analysis possible. There is a need for a comprehensive numerical analysis of the problem to unite together all previous work as special cases, including classical work on liquid jets and columns, and extend the results to parameter values previously unexplored. Numerical work, by its nature, does not have to make any kind of assumptions of the wavenumber, Reynolds number or film thickness. In fact on comparing the results with those from a small wavenumber analysis, it is found that the wavenumber has to be very small for good quantitative agreement and the results diverge quickly.

2. Linear stability analysis

We consider a gravity driven falling film outside a vertical cylinder of radius a, as shown in figure 1. Cylindrical coordinates will be used, with z being vertically downwards and r in the radial direction. The free surface of the liquid is at $r = \zeta$, where $\zeta > a$. Non-dimensional forms of the governing equations will be used with the characteristic velocity being that at the unperturbed free surface and the characteristic length being the unperturbed film thickness. With axisymmetry, the appropriate form of the Orr–Sommerfeld equation in terms of the complex perturbation stream-function amplitude ψ is

$$[(c-u_z)(\mathrm{D}^2-\alpha^2)+\mathrm{D}^2 u_z]\psi = \frac{\mathrm{i}}{\alpha R}(\mathrm{D}^2-\alpha^2)^2\psi, \tag{1}$$

where

$$\mathrm{D}^2 = r\frac{\mathrm{d}}{\mathrm{d}r}\left(\frac{1}{r}\frac{\mathrm{d}}{\mathrm{d}r}\right). \tag{2}$$

c is the complex wave speed, α is the real wavenumber and $u_z(r)$ is the unperturbed fluid velocity. The boundary conditions are

$$\psi = \frac{\mathrm{d}\psi}{\mathrm{d}r} = 0 \quad \text{at } r = \beta, \tag{3}$$

$$\alpha^2\psi + \frac{\mathrm{d}^2\psi}{\mathrm{d}r^2} - \frac{1}{r}\frac{\mathrm{d}\psi}{\mathrm{d}r} - \frac{R}{F^2}\frac{\psi}{c-1} = 0 \quad \text{at } r = 1+\beta, \tag{4}$$

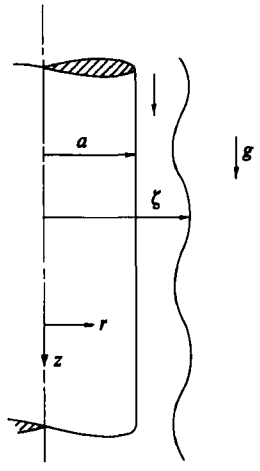

FIGURE 1. Geometry of cylindrical falling film.

$$\alpha(c-1)\frac{\mathrm{d}\psi}{\mathrm{d}r}+\frac{1}{\mathrm{i}R}\left[\frac{\mathrm{d}^3\psi}{\mathrm{d}r^3}-\frac{1}{r}\frac{\mathrm{d}^2\psi}{\mathrm{d}r^2}-\left(\alpha^2-\frac{1}{r^2}\right)\frac{\mathrm{d}\psi}{\mathrm{d}r}\right]$$

$$-\frac{W\psi\alpha}{c-1}\left(\alpha^2-\frac{1}{r^2}\right)+\frac{2\mathrm{i}\alpha^2}{R}\left(\frac{\mathrm{d}\psi}{\mathrm{d}r}-\frac{\psi}{r}\right)=0 \quad \text{at} \quad r=1+\beta. \tag{5}$$

The unperturbed velocity profile is

$$u_z=\frac{2\ln\frac{r}{\beta}-\frac{r^2}{(1+\beta)^2}+\gamma^2}{\gamma^2-2\ln\gamma-1}. \tag{6}$$

In the previous equations the geometrical parameter

$$\beta=\frac{a}{\bar{\zeta}-a}=\frac{\gamma}{1-\gamma}, \tag{7}$$

represents the ratio of the inner radius to film thickness, where the bar over the ζ indicates its unperturbed value and γ is given by

$$\gamma=a/\bar{\zeta}. \tag{8}$$

The Reynolds number R is defined by

$$R=\frac{U(\bar{\zeta}-a)}{\nu}, \tag{9}$$

where ν is the kinematic viscosity and U is the unperturbed fluid velocity at the free surface. The Froude number and Weber number are given by

$$F=U/(g(\bar{\zeta}-a))^{\frac{1}{2}}, \tag{10}$$

$$W=\frac{T}{\rho U^2(\bar{\zeta}-a)}, \tag{11}$$

respectively, where g is the acceleration due to gravity, ρ is the density and T is the surface tension coefficient.

The three independent parameters for the problem are R, W and γ (or β). It can be seen that F is readily obtained from

$$R/F^2 = G, \tag{12}$$

where

$$G = \frac{4(1-\gamma)^2}{\gamma^2 - 2\ln\gamma - 1}. \tag{13}$$

The linear ordinary differential equation (1) and the boundary conditions (3), (4) and (5) constitute an eigenvalue problem for the complex parameter c. Positive, zero or negative imaginary parts of c indicate instability, neutral stability and linear stability respectively.

2.1. *Small wavenumber approximation*

To provide a quantitative basis of comparison for the numerical results, a small wavenumber approximation introduced by Yih (1963) for the flat-plate problem will first be used. We take

$$\psi = \psi_0 + \alpha\psi_1 + \alpha^2\psi_2 + \ldots, \tag{14}$$

and

$$c = c_0 + \alpha c_1 + \alpha^2 c_2 + \ldots. \tag{15}$$

The zeroth-order equation to be solved is

$$\mathrm{D}^4\psi_0 = 0, \tag{16}$$

with the boundary conditions

$$\psi_0 = \frac{\mathrm{d}\psi_0}{\mathrm{d}r} = 0 \quad \text{at} \quad r = \beta, \tag{17}$$

$$\frac{\mathrm{d}^2\psi_0}{\mathrm{d}r^2} - \frac{1}{r}\frac{\mathrm{d}\psi_0}{\mathrm{d}r} - G\frac{\psi_0}{c_0 - 1} = 0 \quad \text{at} \quad r = 1+\beta, \tag{18}$$

$$\frac{\mathrm{d}^3\psi_0}{\mathrm{d}r^3} - \frac{1}{r}\frac{\mathrm{d}^2\psi_0}{\mathrm{d}r^2} + \frac{1}{r^2}\frac{\mathrm{d}\psi_0}{\mathrm{d}r} = 0 \quad \text{at} \quad r = 1+\beta. \tag{19}$$

The first-order equation is

$$\mathrm{D}^4\psi_1 = \frac{R}{\mathrm{i}}\left[4 - \frac{2G}{(1-\gamma)^2}\ln\frac{r}{\beta} + \frac{G(r^2-\beta^2)}{2}\left(1 + \frac{\beta^2}{r^2\gamma^2}\right)\right], \tag{20}$$

with the boundary conditions

$$\psi_1 = \frac{\mathrm{d}\psi_1}{\mathrm{d}r} = 0 \quad \text{at} \quad r = \beta, \tag{21}$$

$$\frac{\mathrm{d}^2\psi_1}{\mathrm{d}r^2} - \frac{1}{r}\frac{\mathrm{d}\psi_1}{\mathrm{d}r} + G(c_1\psi_0 - \psi_1) = 0 \quad \text{at} \quad r = 1+\beta, \tag{22}$$

$$\frac{\mathrm{d}\psi_0}{\mathrm{d}r} + \frac{1}{\mathrm{i}R}\left[\frac{\mathrm{d}^3\psi_1}{\mathrm{d}r^3} - \frac{1}{r}\frac{\mathrm{d}^2\psi_1}{\mathrm{d}r^2} + \frac{1}{r^2}\frac{\mathrm{d}\psi_1}{\mathrm{d}r}\right] + W(1-\gamma)^2\psi_0 = 0 \quad \text{at} \quad r = 1+\beta. \tag{23}$$

Equations (16) and (20) can be easily solved. The eigenvalue c is determined by applying the boundary conditions. The algebra is laborious but straightforward. The result is given by

$$c = 2 + i\alpha R f(W, \gamma), \tag{24}$$

where

$$f = \tfrac{1}{4}G\left[\tfrac{1}{192}G(1+2\beta)^2(41+82\beta+30\beta^2) - \tfrac{1}{8}(1+2\beta+5\beta^2)(3+6\beta+2\beta^2)\right.$$
$$\left. - \tfrac{3}{4}(1+\beta)^2(1+2\beta)\ln\frac{1+\beta}{\beta} + (1+\beta)^4\left(\ln\frac{1+\beta}{\beta}\right)^2\right] - \frac{W}{2(1+\beta)}\left[\tfrac{1}{8}\left(\frac{1+2\beta}{1+\beta}\right)^2 - \frac{1}{G}\right].$$

f is always positive and becomes large near $\gamma = 0$ and 1. It can be seen that the imaginary part of c (and hence the growth rate of the instability wave) depends linearly on R and W. To the order to which the analysis has been carried out, it can be said that the flow is unstable for any set of values of the governing parameters R, W and γ. It should be remembered that the expansions (14) and (15) are valid only if the c_i are at most of order unity. Thus the approximate solution loses validity near $\gamma = 0$ and 1.

3. Numerical technique

In order to obtain detailed information with respect to the instability of the cylindrical falling film, numerical calculations of the eigenvalue problem constituted by equation (1) and conditions (3), (4) and (5) were carried out. The computation scheme was based on that suggested by Davey (1973) for parallel flows and was first tested by checking with his values. In the present case, however, working with relatively low Reynolds numbers is a distinct advantage since computations are much easier than, for example, in boundary-layer flows. Specifically, orthonormalization of the solution vector is not necessary during integration. A straightforward shooting method can be used.

We consider the solution vector to be

$$\boldsymbol{Y} = \left[\psi, \frac{\mathrm{d}\psi}{\mathrm{d}r}, \frac{\mathrm{d}^2\psi}{\mathrm{d}r^2}, \frac{\mathrm{d}^3\psi}{\mathrm{d}r^3}\right]^{\mathrm{T}}. \tag{25}$$

The relation between $\boldsymbol{Y} = \boldsymbol{Y}_0$ at $r = \beta$ and $\boldsymbol{Y} = \boldsymbol{Y}_1$ at $r = 1+\beta$ is defined to be of the form

$$\boldsymbol{Y}_1 = \boldsymbol{B}\boldsymbol{Y}_0, \tag{26}$$

where $\boldsymbol{B}$ is the transfer matrix which depends only on c and not on the boundary conditions. For a given value of c, the differential equation can be integrated from $r = \beta$ to $r = 1+\beta$, using as $\boldsymbol{Y}_0$ the orthonormal vectors $[1,0,0,0]^{\mathrm{T}}$, $[0,1,0,0]^{\mathrm{T}}$, $[0,0,1,0]^{\mathrm{T}}$ and $[0,0,0,1]^{\mathrm{T}}$ in turn. A fourth-order Runge–Kutta scheme with 50 integrations steps was used. The vectors $\boldsymbol{Y}_1$, obtained as a result of these calculations form the columns of $\boldsymbol{B}$.

The first two elements of $\boldsymbol{Y}_0$ are zero from boundary conditions (3). The other two elements are unknown, along with all four of $\boldsymbol{Y}_1$. Six scalar equations can be obtained in these six unknowns, four on using (26) and two from the boundary conditions (4) and (5). A non-trivial solution exists only if the determinant of the system vanishes. The eigenvalue c such that this happens is found by successive interpolation. First

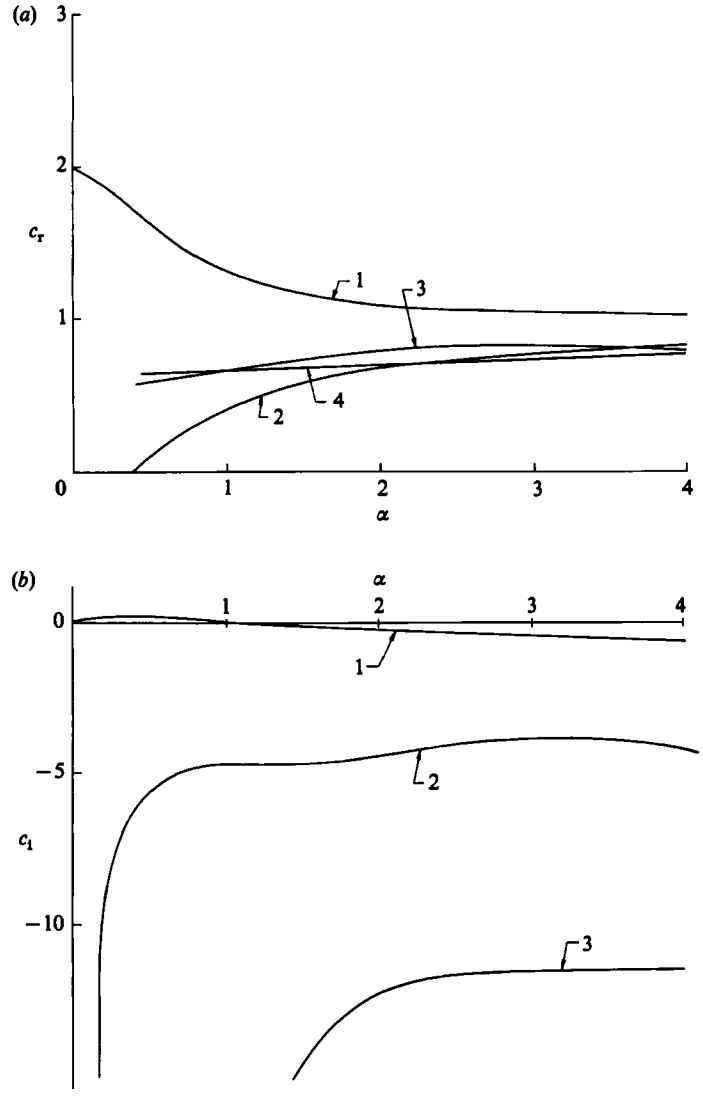

FIGURE 2. (a) c_r and (b) c_i for the low modes with $R = 1$, $W = 1$ and $\gamma = 0.5$. The mode numbers are indicated.

Muller's method and then Lagrange interpolation were used. The former has a larger radius of convergence but is slower, while the latter has a smaller radius but is faster. Normal CPU time on Burroughs 8700 computer for each run was between 4 and 10 seconds, depending on the proximity of the initial guess to the final solution.

4. Numerical results

An infinite but discrete set of eigenvalues can be obtained for a given set of parameters R, α, W and γ. Figure 2 (a, b) shows the real and imaginary parts, c_r and c_i respectively, of the eigenvalues for the low modes as a function of wavenumber for $R = 1$, $W = 1$ and $\gamma = 0.5$. The modes are numbered in order of descending values of the imaginary part. It is seen that only the first mode has any positive imaginary

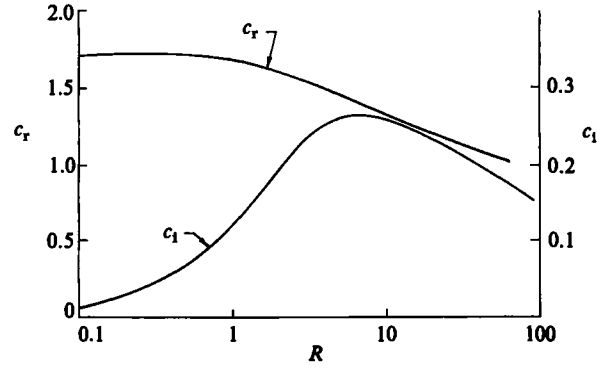

FIGURE 3. c_r and c_i for the most unstable mode for $W = 1$, $\gamma = 0.5$ and $\alpha = 0.4$.

α	Approximate	Numerical
0.4	2+0.305857 i	1.706106+0.118957 i
0.3	2+0.229393 i	1.802386+0.128855 i
0.2	2+0.152929 i	1.896292+0.115599 i
0.1	2+0.076464 i	1.970564+0.070926 i
0.05	2+0.038232 i	1.992367+0.037505 i
0.01	2+0.007646 i	1.999700+0.007641 i
0.005	2+0.003823 i	1.999923+0.003823 i

TABLE 1. Eigenvalue c for different α, with $R = 1$, $W = 1$ and $\gamma = 0.5$

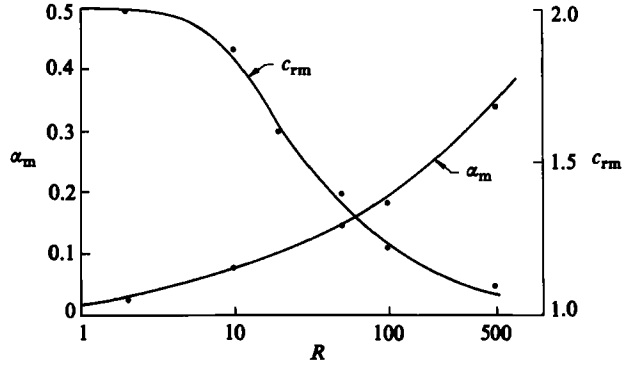

FIGURE 4. Wavenumber α_m and wave speed c_{rm} of most amplified wave for $\gamma = 0.99$. ——, from Pierson & Whitaker (1977); ·····, present work.

part, making this the only mode that is unstable. All perturbations in the wavenumber range $0 < \alpha < \alpha_c$ are amplified. The wavenumber of maximum growth, and hence the most unstable, is indicated by the extremum of c at $\alpha = \alpha_m$.

Figure 3 shows the real and imaginary parts of c for the most unstable mode as a function of the Reynolds number for $W = 1$, $\gamma = 0.5$ and $\alpha = 0.4$. The imaginary part is positive for all R for this particular value of α. c_i is linear with R for small R as predicted by (24) but later drops off sharply.

The value of the numerically computed eigenvalue can be compared to that

J	α_m
1	0.41
2	0.45
4	0.50
8	0.53

TABLE 2. Wavenumber of maximum amplification with $\gamma = 0.015$, $R = 10^{-4}$ and for different $J = WR^2$

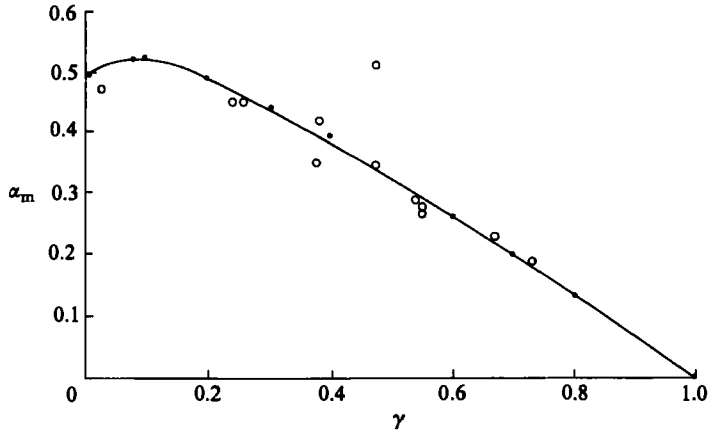

FIGURE 5. Wavenumber of most amplified wave for $R = 10^{-9}$ and $W = 10^9$. ——, theory and ○, experiments of Goren (1962); ●, present work.

obtained from the small wavenumber analysis. Table 1 shows the two sets of eigenvalues for different wavenumbers. There is some difference for moderately small wavenumbers, but the two get closer together as α becomes smaller with the approximate value being always higher. The present approximate analysis does not predict α_c and α_m nor provide the other eigenvalues.

4.1. *Comparison with published data*

As $\gamma \to 1$ from below, the cylindrical geometry tends to that of a vertical flat plate. With the present non-dimensionalization, computation for $\gamma = 1$ is not possible due to singularities. However, the eigenvalues of the lowest mode tend to a constant as $\gamma \to 1$. In this way flat-plate values can be obtained and comparison made with published results. For $\gamma = 0.99$, calculated values of the critical wavenumber α_c were about 5% higher than those found by Whitaker (1964), but coincide exactly with those of Sternling & Barr-David reported in that paper. For the same γ, figure 4 shows the wavenumber α_m and wave speed c_{rm} of the most amplified wave. It is in good agreement with the results of Pierson & Whitaker (1977), who have checked their values against those obtained theoretically and experimentally by other authors.

In the other limit, as $\gamma \to 0$, a cylindrical jet with a vanishingly thin solid core is obtained as a limit. Even in this limit, there are physical differences with respect to a cylindrical falling jet. The latter is strictly speaking always accelerating. The velocity profile is also different in a vanishingly small region due to different

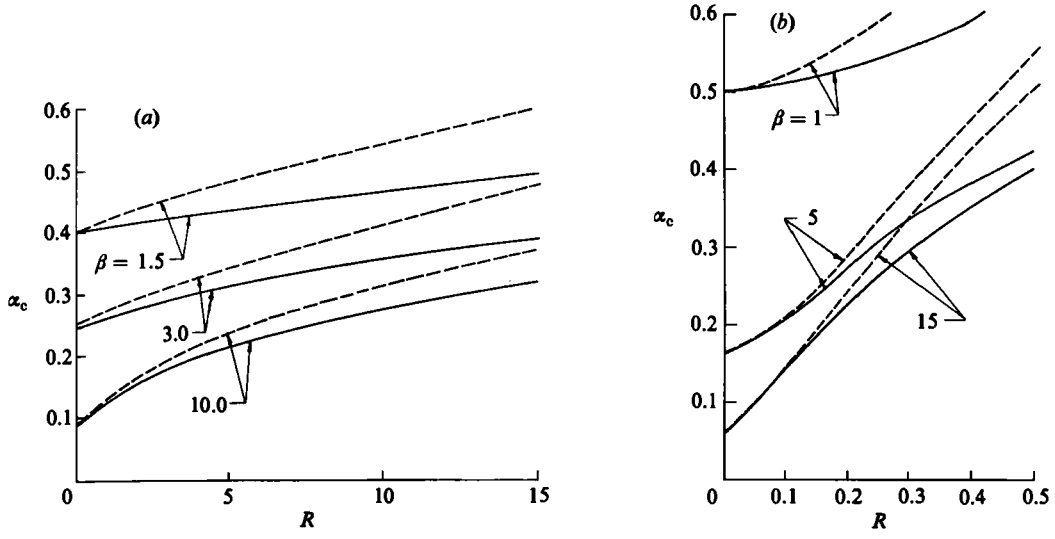

FIGURE 6. Comparison of neutral stability curves. ——, present work; – – –, from (*a*) Lin & Liu (1975) for $W = 100$ and (*b*) Krantz & Zollars (1976) for their parameter $N_\zeta = 2$.

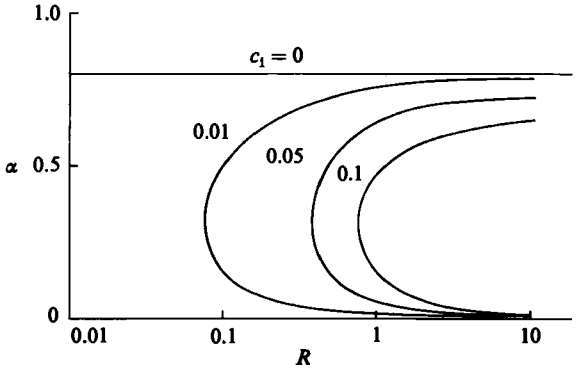

FIGURE 7. Wave amplification curves for $W = 1$ and $\gamma = 0.5$.

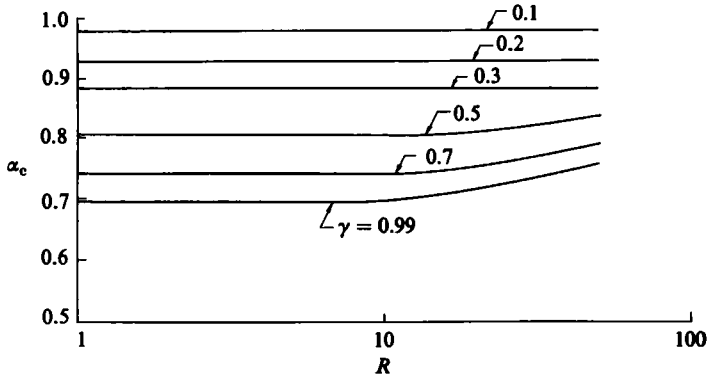

FIGURE 8. Neutral stability curves for $W = 1$.

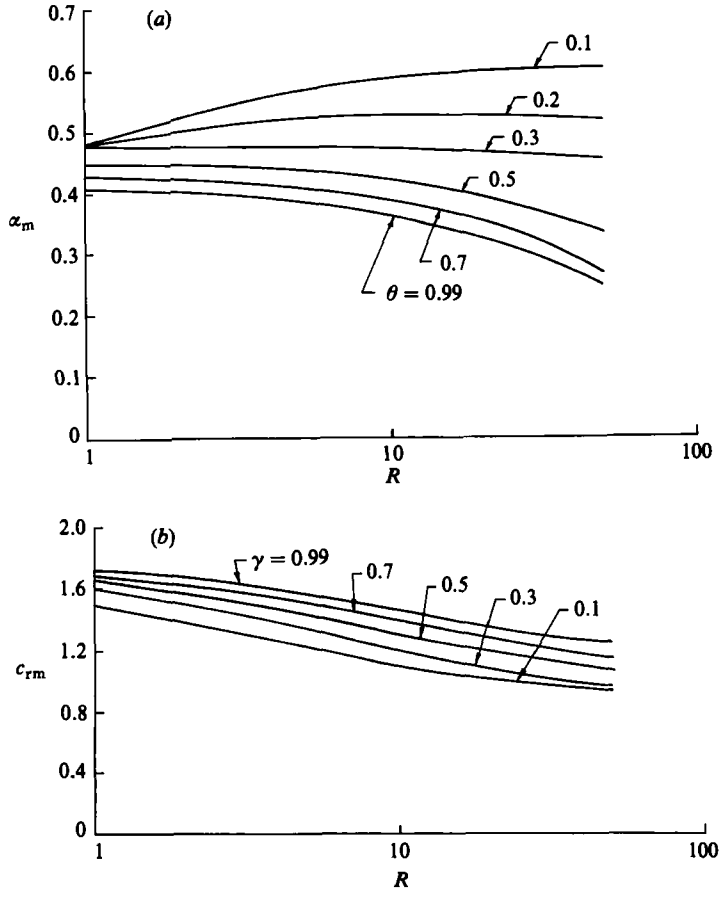

FIGURE 9. (a) Wavenumber α_m and (b) wave speed c_{rm} of most amplified wave for $W = 1$.

boundary conditions. However, the stability characteristics seem to be similar and the results obtained here for $\gamma \to 0$ can be compared to those for a static water column for which considerable information exists. The analysis presented by Chandrasekhar (1961) does not make a high-viscosity approximation and is hence more general than that of Rayleigh (1879, 1892). Table 2 shows the wavenumber for maximum amplification with $\gamma = 0.015$. We have taken $W \to \infty$ and $R \to 0$ such that $J = WR^2$ is a constant; the value of R was fixed at 10^{-4} and W varied accordingly. The results for different J are close to the values given in Chandrasekhar (1961) for a static column. They compare favourably also with the values obtained from

$$\alpha_m = \frac{0.707}{\left[1+\left(\frac{9}{2J}\right)^{\frac{1}{3}}\right]^{\frac{1}{2}}}, \tag{27}$$

proposed by Weber (1931).

Detailed comparison for all values of γ can also be made with the calculations of Goren (1962). His assumptions correspond to a value of $R = 0$, so we have taken $R = 10^{-9}$ and $W = 10^9$. Figure 5 shows the wavenumber of the most amplified wave α_m as a function of γ. Once again the agreement is good. Also indicated are experimental data reported in that paper converted to the present notation.

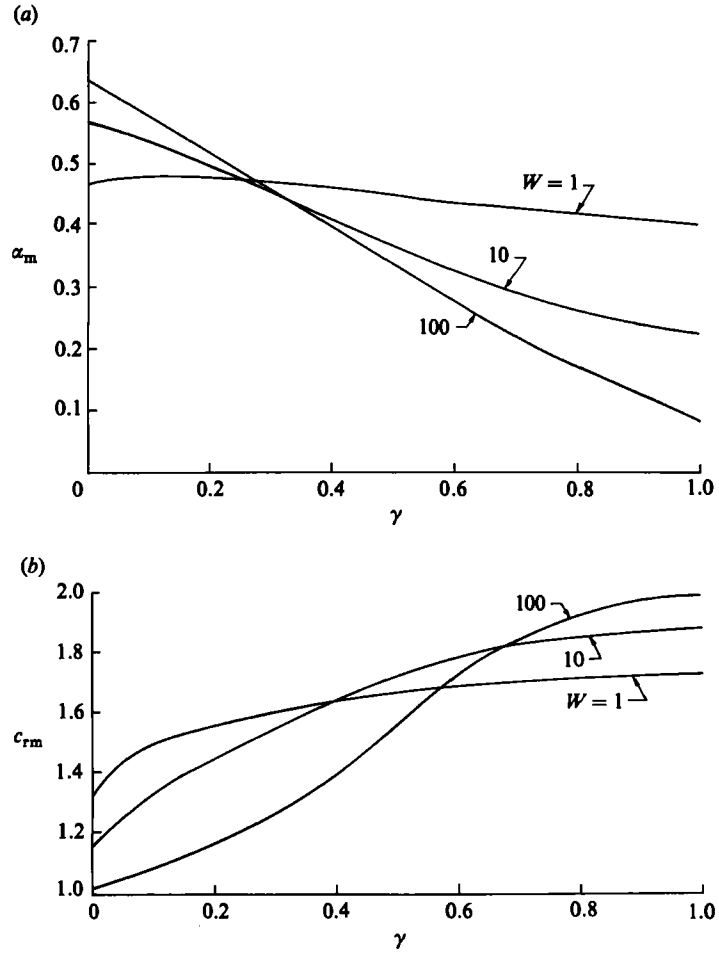

FIGURE 10. (*a*) Wavenumber α_m and (*b*) wave speed c_{rm} of most amplified wave for $R = 1$.

Figure 6(*a*, *b*) shows the difference between the neutral stability curves calculated by the approximation of Lin & Liu (1975) and Krantz & Zollars (1976) respectively, compared to the present numerical method. The differences are accentuated as the Reynolds number and hence critical wavenumber increase. The latter also increases with the relative thickness of the film, i.e. for vanishing β. For large β, as in the experiments of Binnie (1957) where $\beta = 118.64$ and $W = 597$, the difference practically disappears.

4.2. *Cylindrical-film numerical results*

For highly curved cylinders with thick films and for large Reynolds numbers, the approximate theories do not give satisfactory results and numerical methods have to be applied. Figure 7 shows the constant amplification curves for $W = 1$ and $\gamma = 0.5$. For moderately large R, all wavenumbers under 0.8 are amplified. As $R \to 0$, the critical wavenumber goes to zero very quickly. The amplification rate increases with R. Figure 8 shows the critical wavenumber as a function of R. For small R the critical wavenumber is practically a constant but increases with the curvature of the film. Figure 9(*a*, *b*) shows the wavenumber and wave speed of the most amplified wave as

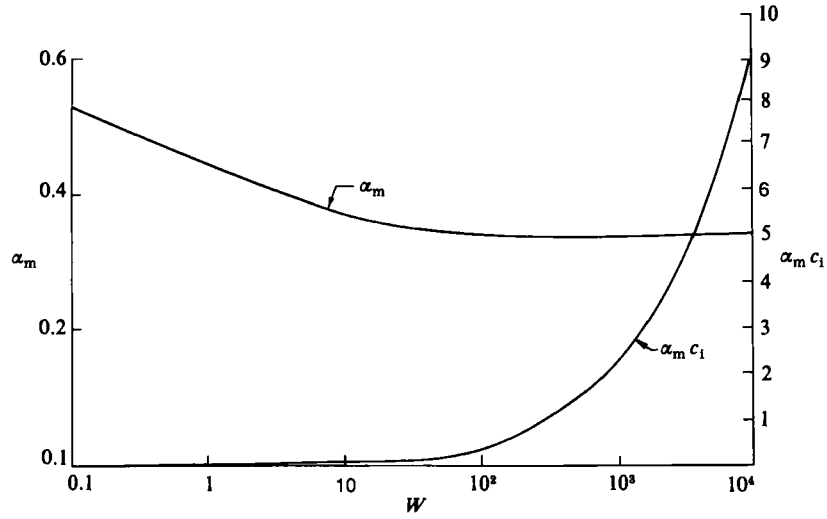

FIGURE 11. Wavenumber α_m and amplification rate $\alpha_m c_i$ of most amplified wave for $R = 1$ and $\gamma = 0.5$.

a function of Reynolds number with $W = 1$. α_m increases on increasing film curvature. Thus, for the same liquid surface velocity and film thickness around a cylinder and over a flat plate, smaller wavelength instabilities would appear on the cylindrical film. A change in Reynolds number produces an ambiguous effect, if the other parameters are kept constant. Figure 9(*a*) shows that increasing R signifies an increase or decrease in the wavenumber of the most amplified wave depending on whether γ is $<$ or $>$ about 0.25.

In Figure 10(*a*, *b*), the most unstable wave is analysed as a function of γ. The effect of surface tension here is curious. For γ less than about 0.25, increasing Weber numbers increases its wavenumber while for larger γ, the effect is the opposite. However, as $W \to \infty$, α_m tends to an asymptotic value α_m^* as indicated in figure 11. It decreases first since $\gamma > 0.25$. α_m^* varies little with R, but strongly with γ. The rate of amplification $\alpha_m c_i$ is also shown in the figure.

5. Conclusions

The linear stability of the cylindrical falling film has been previously studied using analytical techniques and with various approximations which restrict the usefulness of the results obtained. The present numerical method confirms the fact that the film is unstable to perturbations with wavenumbers ranging from zero to a critical value for all Reynolds numbers, Weber numbers and radius ratios. However, quantitative values of the critical wavenumbers and amplification rates can be significantly different from that predicted by an approximate theory. This is important for any experimental verification. Qualitatively, growth rates are not linear with Reynolds numbers nor with Weber numbers as predicted by a first-order theory. With increasing curvature of the film the range of unstable wavenumbers and the wavenumber of the most amplified wave increase. For low γ the wavenumber of the most amplified wave increases with Reynolds numbers or Weber numbers while for high γ it decreases.

Revision of the manuscript was carried out while one of the authors (M. S.) was on sabbatical leave at Cornell University. His thanks go to Professor K. E. Torrance and the Sibley School of Mechanical and Aerospace Engineering for their hospitality during this period.

REFERENCES

ATHERTON, R. W. & HOMSY, G. M. 1976 On the derivation of evolution equations for interfacial waves. *Chem. Engng Commun.* **2**, 57–77.

BINNIE, A. M. 1957 Experiments on the onset of wave formation on a film of water flowing down a vertical plane. *J. Fluid Mech.* **2**, 551–553.

BENJAMIN, T. B. 1957 Wave formation in a laminar flow down an inclined plane. *J. Fluid Mech.* **2**, 554–574 (see also Corrigendum 1958, *J. Fluid Mech.* **3**, 657).

BRUIN, G. J. DE 1974 Stability of a layer of liquid flowing down an inclined plane. *J. Engng Maths* **8**, 259–270.

CHANDRASEKHAR, S. 1961 *Hydrodynamic and Hydromagnetic Stability*. Clarendon.

DAVEY, A. 1973 A simple numerical method for solving Orr–Sommerfeld problems. *Q. J. Mech. Appl. Maths* **26**, 401–411.

GOREN, S. L. 1962 The instability of an annular thread of fluid. *J. Fluid Mech.* **12**, 309–319.

HOMSY, G. M. & GEYLING, F. T. 1977 A note on instabilities in rapid coating of cylinders. *AIChE J.* **23**, 587–590.

KAPITZA, P. L. & KAPITZA, S. P. 1949 Experimental study of undulatory flow conditions. *Zh. Eksp. Teor. Fiz.* **19** (see *Collected Papers of P. L. Kapitza*, 1964, pp. 690–709. Macmillan).

KRANTZ, W. B. & GOREN, S. L. 1971 Stability of thin liquid films flowing down a plane. *Ind. Engng Chem. Fundam.* **10**, 91–101.

KRANTZ, W. B. & ZOLLARS, R. L. 1976 The linear hydrodynamic stability of film flow down a vertical cylinder. *AIChE J.* **22**, 930–938.

LIN, S. P. & LIU, W. C. 1975 Instability of film coating of wires and tubes. *AIChE J.* **21**, 775–782.

PIERSON, F. W. & WHITAKER, S. 1977 Some theoretical and experimental observations of the wave structure of falling liquid films. *Ind. Engng Chem. Fundam.* **16**, 401–408.

RAYLEIGH, LORD 1879 On the capillary phenomenon of jets. *Proc. R. Soc. Lond.* **29**, 71–97.

RAYLEIGH, LORD 1892 On the instability of a cylinder of viscous liquid under capillary forces. *Phil. Mag.* **34**, 145–154.

SHLANG, T. & SIVASHINSKY, G. I. 1982 Irregular flow of a liquid film down a vertical column. *J. Phys. Paris* **43**, 459–466.

WEBER, C. 1931 Zum Zerfall eines Flussigkeitsstrahles. *Z. angew. Math. Mech.* **11**, 136–141.

WHITAKER, S. 1964 Effect of surface active agents on the stability of falling liquid films. *Ind. Engng Chem. Fundam.* **3**, 132–142.

YIH, C.-S. 1954 Stability of parallel laminar flow with a free surface. *Proc. 2nd U.S. Natl Congr. Appl. Mech. ASME*, pp. 623–628.

YIH, C.-S. 1963 Stability of liquid flow down an inclined plane. *Phys. Fluids* **6**, 321–334.

YIH, C.-S. 1969 *Fluid Mechanics*. McGraw-Hill.